OPERATIONAL MATHEMATICS SERIES NO. 5

A SET OF ANGLES OF OBLIQUITY FOR USE IN ASSESSING BODY ARMOR

FEBRUARY 1961

DEPARTMENT OF THE ARMY
OFFICE OF THE QUARTERMASTER GENERAL

A SET OF ANGLES OF OBLIQUITY FOR USE IN ASSESSING BODY ARMOR

by

Herbert Maisel
Wallace Chandler
Gerald DeCarlo

February 1961

OPERATIONAL MATHEMATICS SERIES
REPORT NO. 5

FOREWORD

In developing clothing for a modern army, the Quartermaster Corps must consider current battlefield requirements. Personnel armor, shielding the combat soldier from fast-flying fragments, is a case in point, for its success clearly hinges on its battlefield effectiveness. As this battlefield effectiveness cannot be tested directly, it must be analytically assessed using the tools of modern mathematics. In the course of this assessment it is necessary to incorporate realistic values for the angle at which the fragment strikes the armor, the angle of obliquity, since this angle affects the penetrability of the fragment. Quartermaster mathematicians in the Operational Mathematics Office, therefore, studied this problem in order to make a realistic determination of the relative frequency of different values of the angle of obliquity. Their work is reported in this, the fifth report in the Quartermaster Operational Mathematics Series.

C. G. Calloway

C. G. CALLOWAY
Major General, USA
Director of Operations

Table of Contents

LIST OF TABLES AND FIGURES

ABSTRACT

Measures of the effectiveness of body armor have been obtained in the past assuming the angle of obliquity is zero, i.e., that the projectiles strike the armor normal to its surface. Since penetrability is a function of the angle of obliquity, it is important to determine the set of angles likely to be encountered and to use this set when assessing body armor. An estimate of the distribution of the angles of obliquity was obtained for fragments striking the upper torso. It turned out in this situation that the proportion of angles of obliquity less than X degrees is approximately 2X% for $0 \leq X \leq 40$, $(X + 40)\%$ for $40 \leq X \leq 60$ and 100% for $X \geq 60$. The procedure used to obtain this estimate is directly applicable to making similar estimates for other parts of the body.

ACKNOWLEDGEMENTS

The authors wish to thank Messrs. Vincent Thomas and Frank Urban of the Services Office of the Research & Engineering Division, OQMG, for their assistance in obtaining the manikins and clothing used in this study, and Dr. T. N. E. Greville of the Operational Mathematics Office for his technical assistance in the smoothing of the data.

INTRODUCTION

The angle of obliquity at which a projectile strikes a target is known to affect penetrability. In evaluating body armor for field use it is consequently important to know the angles of obliquity likely to be encountered in the field . In the past it has been assumed that most fragments from a shell exploding at a distant point would tend to strike the target at angles close to the normal. However, this assumption has never been substantiated.

The particular target of concern here is a human figure wearing a combat uniform and a protective body armor vest. The question might be stated simply as follows: If the target were repeatedly exposed to projectiles from the explosion of a fragmenting shell, and we could measure the angles of obliquity of the projectiles striking the target, what is a likely distribution of the magnitudes of these angles? Since it is impractical to measure such angles in laboratory or field firing tests, a mathematical technique that would estimate the distribution was desired. This report summarizes the work done on this question by the Operational Mathematics Office of the Quartermaster Corps.

In attacking this problem, it is necessary to limit the discussion to a particular region of the target. In this report this region is the upper chest, more specifically, a narrow band about the body slightly below armpit level. The same techniques could be applied to other regions of the body as well.

The angle of obliquity is the angle between the normal to the target surface and the tangent to the projectile trajectory, both taken at the point of impact. This is, of course, a three-dimensional problem. Our analysis was made using a two-dimensional model. In this reduced case, the target is a plane figure: the shape of the clothed human figure as it would appear in a horizontal cross-section at the level of the body we are studying. The normal and the tangent are represented by their respective projections in the horizontal plane of the cross-section. The angle of obliquity we will deal with then is the projection in the horizontal plane of the true angle.

This reduction in dimension is a major simplification. However, any error so introduced need not be major. When reasonable conditions, limiting the deviation of the true trajectory from the horizontal plane, are specified, the discrepancy between the true angle and its projection can be shown to be small. The magnitude and direction of this error under specific conditions are discussed on pages 17 - 20 . A general discussion of the

geometrical relationship between the true and the projected angle is given in Appendix II.

To apply the technique described here, it is necessary to specify the distance, in the horizontal plane, from the target to the projected point of the explosion. Distributions will be estimated for two distances, 40 and 100 feet.

The remainder of this report is divided into seven major sections. The first contains a description of the geometrical model used in the study, the second a description of the procedure used to obtain the distribution of the angles of obliquity. The distribution arrived at is presented in the third section and a discussion of the accuracy of some aspects of the procedure is given in the fourth one. This discussion appears after the results because some of the results are used in the course of the discussion. A comparison of our results with those one would obtain using further simplifying assumptions is given in the fifth section. The sixth and seventh sections contain conclusions and recommendations, respectively.

THE GEOMETRICAL MODEL

In constructing a model, the first question to be asked is: What is the nature of the conditions that may be found in the field? We will prescribe three conditions. First, to make the problem manageable, we will consider the target only in an upright, exposed position. Second, we will permit the target to turn in all possible directions with respect to the detonation, i.e., facing it, with his back turned, etc., and will assume that each of these is equally likely. Third, we will consider only those projectiles with trajectories that would have intersected the body if no armor or clothing were present.

The geometrical model used in our study will now be described. As indicated earlier this model lies entirely in the horizontal plane containing the cross-section of the target under study. The basic elements of the model are the target, the projected trajectory, projected normal, projected angle of obliquity, and two angles that will be used to specify the relation of the trajectory to the target. The elements and their relationships are shown in Figure 1; they will be discussed in more detail in the succeeding paragraphs.

The first important element of the model is a pair of cross-sections, one within the other; the outer one is the cross-section of the fully clothed man, the inner one that of the unclothed man.

A second element is the projection in the horizontal plane of the point of explosion and the fragment trajectories originating from it. We will call this projected point of explosion the source. It is located at some distance d from the center of the cross-section.

Three assumptions about the projection of the trajectories were made, namely:

1. that the trajectories will project as straight lines. This is equivalent to ignoring wind or other forces which might cause a fragment to move laterally as well as vertically. Note that since movement is only in a vertical plane, the tangent to the trajectory at the point of impact will project into the same straight line as the trajectory, so that the projected angle of obliquity is the angle between the projected normal to the surface and the projected trajectory itself.

2. the radial distribution of the projected trajectories about the source is uniform.

Figure 1. The Geometrical Figure

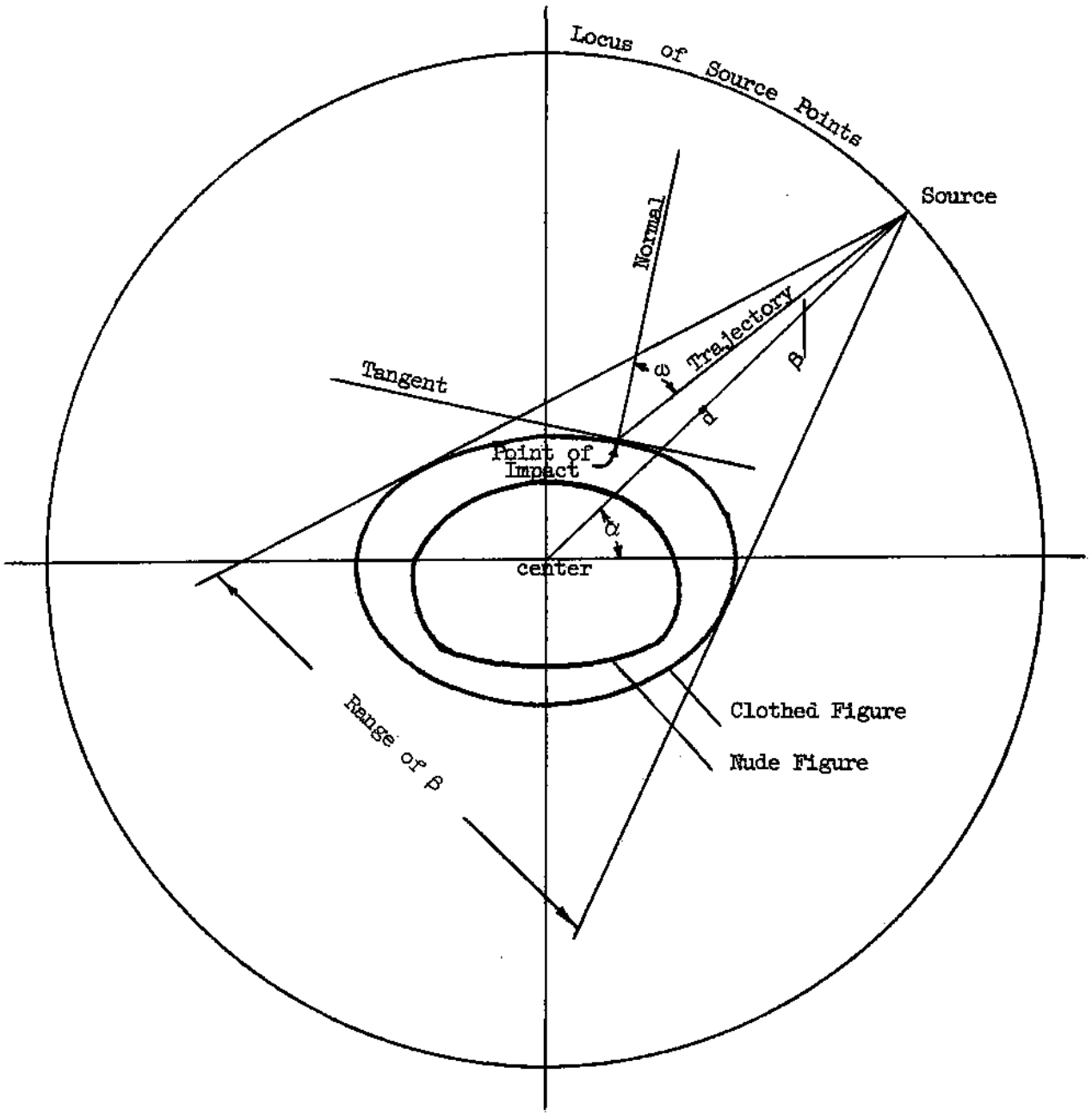

3. the true trajectory continues in the same vertical plane after penetrating the clothing, i.e., the projected trajectory continues in a straight line. This assumption is known to be valid for small angles of obliquity and though the available evidence for larger angles indicates the projectiles may turn, it is not to be expected that in the long run turns in one direction will exceed those in the other, so that our assumption is not unreasonable. Of course, although we only wish to consider those trajectories intersecting the inner figure, the angle of obliquity we seek is the angle made with the outer figure.

In order to describe the last elements -- the two angles specifying the trajectory -- we require Figure 1. So as to simplify this discussion, the terms normal, trajectory, and angle of obliquity, will be used to refer to their respective projections in the horizontal plane.

The exact shape of the cross-sectional figures and the method used to obtain them will be discussed in Section III. For the moment we can think of a general cross-sectional figure, somewhat broader than it is deep. It is helpful to think of a co-ordinate axis system superimposed on the figure so that the origin coincides with the "center" of the cross-section. A precise definition of the term center will be given later.

We will call the line joining the center of the figure to the source, the source line. Suppose, while holding the figures, including the axes and the center, fixed we allow the source to move along the circumference of a circle of radius d. In this manner the figure can assume any desired orientation toward the source -- facing it, turned sidewise, etc. This orientation may be measured by the angle, called alpha, between the source line and the x-axis. In our model we assume all values of α are equally likely.

The angle between the source line and the trajectory we have called beta. Each value for β determines a specific trajectory. Of course, only those values of β within a narrow range to either side of the source line will determine trajectories which intersect the inner figure. Since we have assumed that the trajectories are radially distributed about the source in a uniform manner it follows that all values of β are equally likely.

PROCEDURE

Summary. In general, the procedure was to first determine the size and shape of the cross-section of the armored man (the outer figure) and

the nude man (the inner figure). Then a representative set of trajectories are specified in terms of α and β and the trajectories are drawn full scale on a sheet of graph paper near their intersection with the figures -- the inner and outer figure were previously drawn on the same graph paper. The tangent at the point of impact is drawn and the angle of obliquity, ω, measured directly using a protractor. This was done for a random sample of 180 trajectories and the results were combined and smoothed to obtain an estimate of the distribution of the angles of obliquity. The procedure will now be described in more detail and a numerical example worked to illustrate its use.

The Size and Shape of the Cross-Sections. The shape of the outer figure was determined using a manikin dressed in a regulation cold-wet uniform with a body armor vest as the outer garment. The layers of clothing -- heavy, woolen underwear, woolen shirt, field jacket, and armor vest -- provided a padding of one to two inches about the body, considerably altering the shape from that of the unclothed manikin. A life-size, representative cross-section of the clothed manikin was reproduced on a sheet of graph paper. This was done by taking measurements of the manikin with respect to several base lines, as described below.

The reader is referred to Figure 2. The sheet of paper represents the horizontal plane of the cross-section. A vertical plane, bisecting the manikin into symmetric right and left halves, would intersect the horizontal plane in a straight line, which we will call the y-axis. If we now hold two rulers in the horizontal plane perpendicular to the vertical plane, and tangent to the outer surface of the clothed manikin, we establish two base-lines. The distance between these two parallel rulers is the depth of the outer figure. In this case, the depth was 13 inches. We will call these lines the anterior and posterior base lines. A third parallel line, midway between these two is also drawn. This we will call the x-axis. The center is the intersection of the x- and y-axes.

The next step is to make a series of measurements of the distances from the ruler to the body surface, symmetrically, at one-inch intervals to the right and left of the midpoint of the anterior base line. A few additional measurements are made near the left and right hand edges because of the extreme curvature there. Since it is reasonable to think of the human body as symmetric from left to right, the two symmetric measurements are averaged. A summary of the actual and averaged measurements is given in Table 1. These average measurements are then plotted on the graph paper full scale with the same relationship to the anterior base line as they had to the ruler. The same procedure is followed with

Figure 2. The Inner and Outer Figures
Scale: 1/2 inch = 1 inch

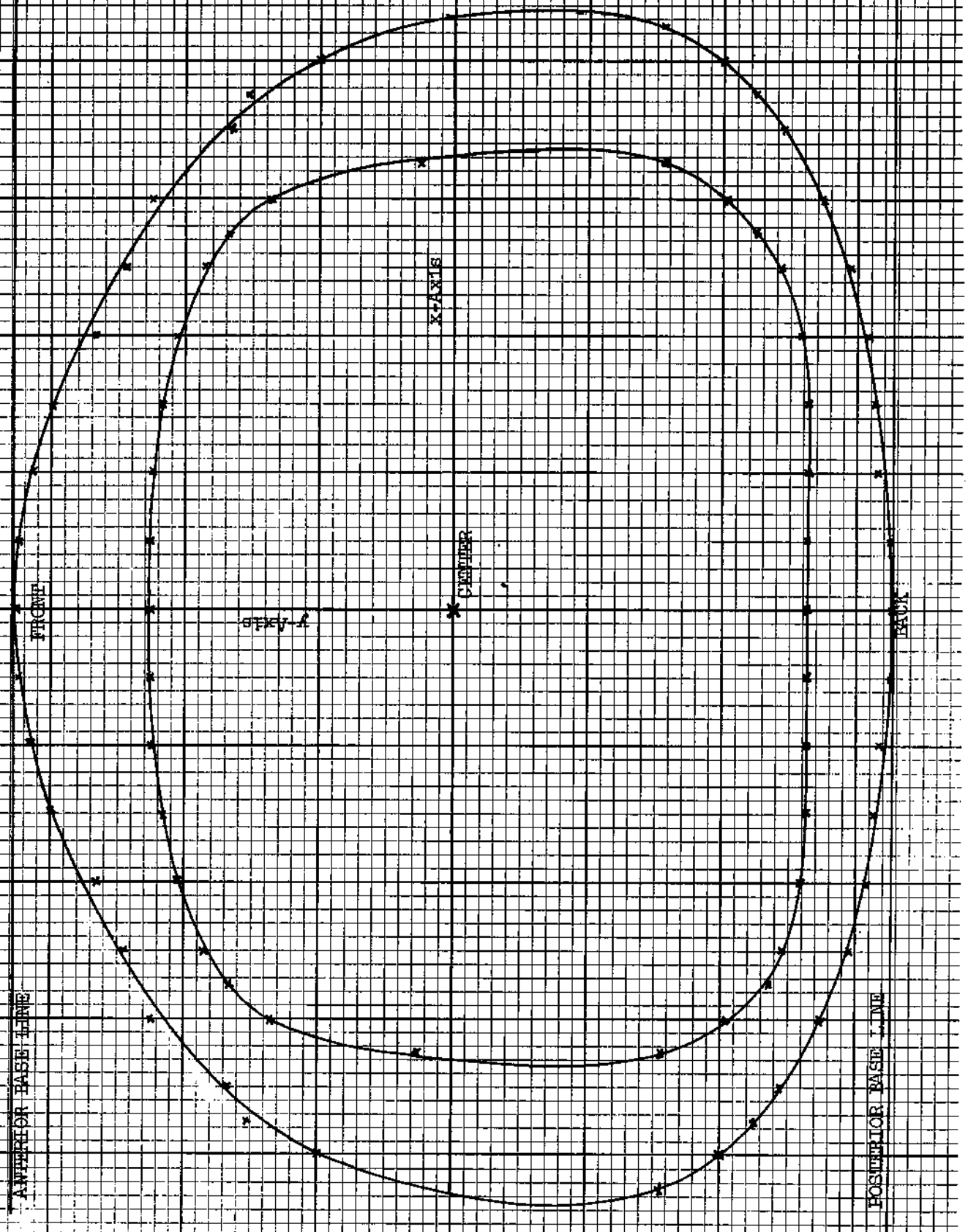

44674

respect to the posterior base line. The breadth is measured by holding rulers at the side of the body and measuring the distance between the parallel rulers. This distance was found to be 17-1/2 inches. To represent this, two lines, parallel to the y-axis and 8-3/4" to the right and to the left of it are drawn. We call these the left and right base lines. A smooth curve through the plotted points is inscribed in the rectangle formed by the four base lines. This is the cross-section of the clothed man. The same technique can be used to obtain a representative cross-section of the unclothed figure. This inner figure has a depth of 9.75" and a breadth of 13.5". On the basis of these measurements, our manikin would appear to be slightly larger through the chest than the average male soldier as revealed in statistical studies.[1] However, the difference is small, and our measurements fall well within the range of measurements recorded in these studies.

The somewhat rectangular shape of the cross-section may be a surprise to some readers. This shape is corroborated by Anatomy texts illustrating actual cross-sections of the human body.[2]

The inner figure was positioned so that the space between the two figures (representing the thickness of the clothing layer) was approximately the same at the four "corners". This thinnest clothing layer can be seen from the drawing to be about 1". At the back, the space is about 1.5", and at the sides and the front about 2".

Specifying the Trajectories -- α and β. Having established the shape of the target we now must determine the trajectories. The angles α and β are used for this purpose. Referring again to Figure 1, because of the left-right symmetry of the figure, we can confine our discussion to, say, the right half of the circle so that α will vary from -90° to $+90^{\circ}$. Recall that all values of alpha within this range are equally likely.

Fixing α only a small proportion of the trajectories will intersect the inner figure. We wish to confine our discussion to only these trajectories. Because these trajectories lie within a narrow range to either side of the source line, it is most convenient to define the measurement of the angle beta in positive and negative directions from the source line. Angles beta in a clockwise direction will be considered negative -- those in a

---

[1] Hooten, E. A., Body Build in a Sample of the United States Army. Technical Report EP-102, Environmental Protection Research Division, Headquarters, QM Research & Engineering Command, US Army, Natick, Massachusetts. February 1959.

[2] Eycleshymer, A. C. and Schoemaker, D. M. A Cross-Section Anatomy. D. Appleton and Co., New York. 1911.

Table 1. Measurements Used to Obtain the Cross-Sectional Figures, In Inches

OUTER FIGURE

Front				Back			
Left Depth Meas.	Inches From Center	Right Depth Meas.	Av.	Left Depth Meas.	Inches From Center	Right Depth Meas.	Av.
0	0	0	0	0	0	0	0
0	1	0	0	0	1	0	0
3/8	2	1/4	5/16	1/8	2	1/4	3/16
1/2	3	1/2	1/2	3/16	3	3/8	1/4
1-5/16	4	7/8	1-1/16	5/16	4	5/16	5/16
1-7/16	5	1-5/16	1-3/8	1/2	5	3/4	5/8
1-15/16	6	2-5/8	2	1-5/16	6	1-1/16	1
2-15/16	7	3-1/4	3-1/16	1-9/16	7	1-3/4	1-5/8
3-5/16	7.5	3-9/16	3-7/16	2-1/16	7.5	1-15/16	2
4-3/16	8	4-3/4	4-1/2	2-3/4	8	2-5/16	2-1/2
				3-7/16	8.5	3-1/4	3-3/8

INNER FIGURE

Front				Back			
Left Depth Meas.	Inches From Center	Right Depth Meas.	Av.	Left Depth Meas	Inches From Center	Right Depth Meas.	Av.
0	0	0	0	0	0	0	0
0	1	0	0	0	1	0	0
0	2	0	0	0	2	0	0
1/8	3	1/8	1/8	0	3	0	0
3/8	4	5/16	3/8	1/16	4	1/16	1/16
3/4	5	11/16	3/4	3/8	5	7/16	3/8
1-1/8	5.5	1-1/16	1-1/8	5/8	5.5	13/16	3/4
2	6	1-1/2	1-3/4	1-1/16	6	1-1/4	1-1/8
	6.5	4	4	2-1/4	6.5	2-1/16	2-1/8

counterclockwise direction, positive. The limiting value of beta in either direction is the value determining the trajectory tangent to the inner figure. These negative and positive limits define the range of beta for a fixed value of alpha. The range of beta will be different for different values of the angle alpha, e.g., the range of beta for $\alpha = 0^{\circ}$ is obviously smaller than for $\alpha = 90^{\circ}$.

At a given distance d, assigning values to the pair of angles α and β, each within the range just defined, will generate a trajectory. We can draw any trajectory on the graph paper and find its point of intersection with the cross-sectional figure in the following manner: Given α, β, and d, the intercepts of the trajectory with the co-ordinate axes can be computed. For positive α and β, using the Law of Sines, we see from Figure 3 that for a, the x-intercept,

$$\frac{d}{\sin(\alpha + \beta)} = \frac{a}{\sin \beta} \quad .$$

Therefore,

$$a = \frac{d \sin \beta}{\sin(\alpha + \beta)} \quad .$$

The y-intercept, b, is then obtained from the relation

$$\frac{-b}{a} = \tan(\alpha + \beta), \text{ which gives, } b = -a \tan(\alpha + \beta).$$

FIGURE 3. Estimating the Intercepts

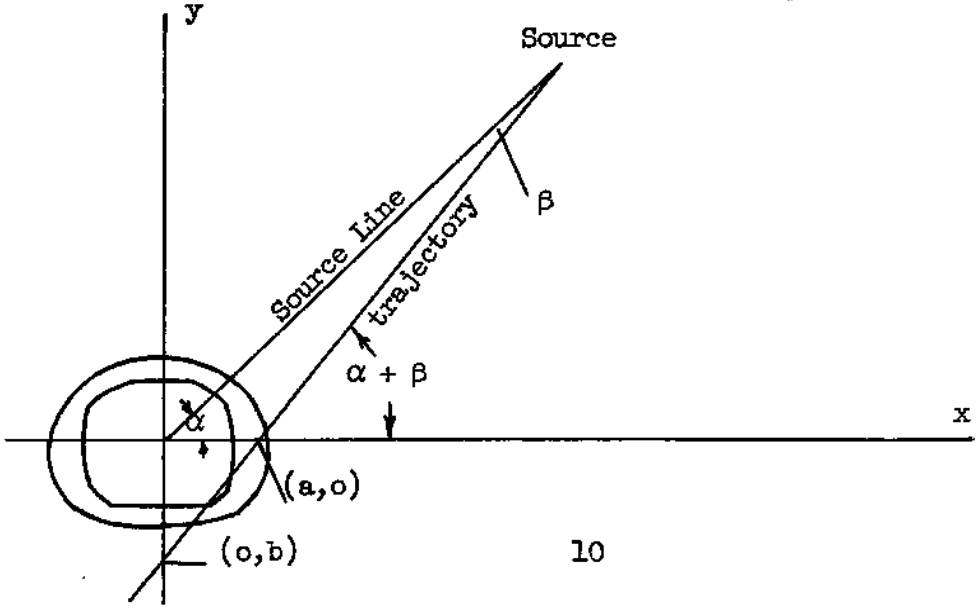

Careful analysis will show that these relationships hold for all combinations of negative and positive α and β. Only in two special cases is either of the intercepts undefined. This occurs when $|\alpha| = |\beta|$ or $|90-\alpha| = |\beta|$ in which cases the trajectory is parallel to one axis and does intersect the other. Of course, the trajectory can still be drawn since the above formulas can be used to compute the intercept with the axis it does intersect.

The Range of β. We are now in a position to construct a trajectory given α and β and measure the resultant angle of obliquity. All that remains then is to choose suitable values of α and β. In order to do this we must be able to estimate the range of β given α. This was done for each of the two values of d by first selecting several values of α in the range -90° to $+90^{\circ}$, then working out the minimum and maximum values of β possible for each α, and finally plotting these results as a function of α and drawing a smooth curve through them. Given any α in the range -90° to $+90^{\circ}$ we can use these curves to read off the corresponding values for the maximum and minimum β. The curves are shown as Figures 4 and 5.

How then do we estimate the minimum and maximum values of β associated with a certain α, say α_o. A first estimate is made by measuring the greatest distance from the source line corresponding to α_o to the edge of the inner figure along lines perpendicular to this source line. This is most easily done by sliding a ruler along the appropriate source line perpendicular to it. The first estimate then is the angle whose tangent is this distance divided by d. Using this value for β and α_o we may construct a trajectory. if this trajectory is indeed tangent to the inner figure our job is done; if not we adjust the first estimate of β in accordance with the observed trajectory. The second estimate is almost always satisfactory.

Sampling -- Choosing α and β. Now we come to the choice of α and β. It has been mentioned that all values of these angles within their respective ranges are equally likely. This must be taken into account in selecting values for our sample of trajectories. For alpha, this is easily done by selecting values evenly distributed over the range -90° to $+90^{\circ}$, as we have done. A complete list of the values of α used is given in Appendix I.

The choice of β is more complex. For each value of α a value of β must be selected so that 180 values of beta must be chosen and assigned to α in a random manner. This was done by first assigning a 3-digit number from a table of random numbers[3] to each of the 180 values of alpha. If we think

[3]The Rand Corp. A Million Random Digits with 100,000 Normal Deviates, The Free Press Publishers, Glencoe, Illinois, 1955.

Figure 4. Limits of β as a Function of α
for d = 40 Feet

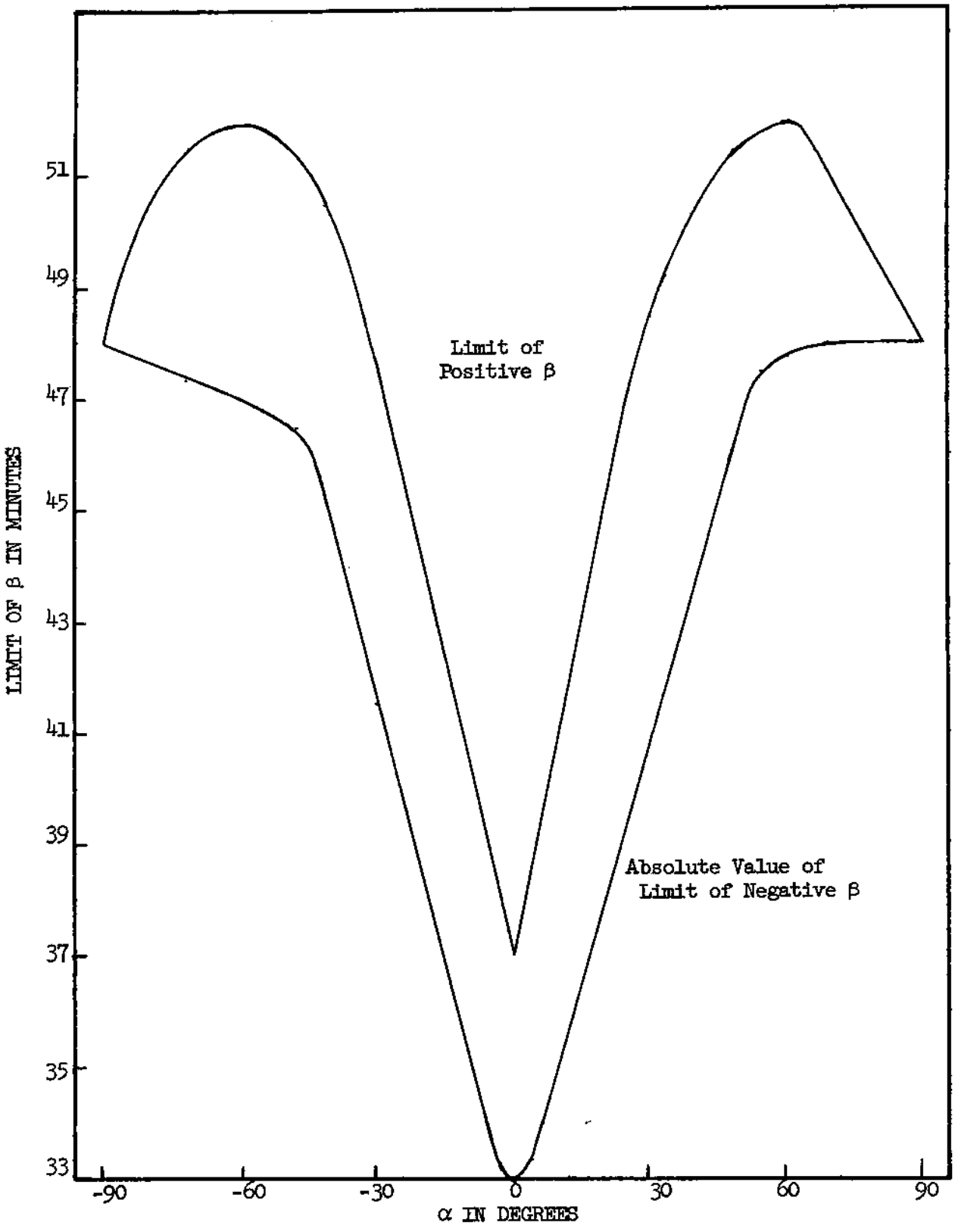

Figure 5. Limits of β as a Function of α for d = 100 Feet

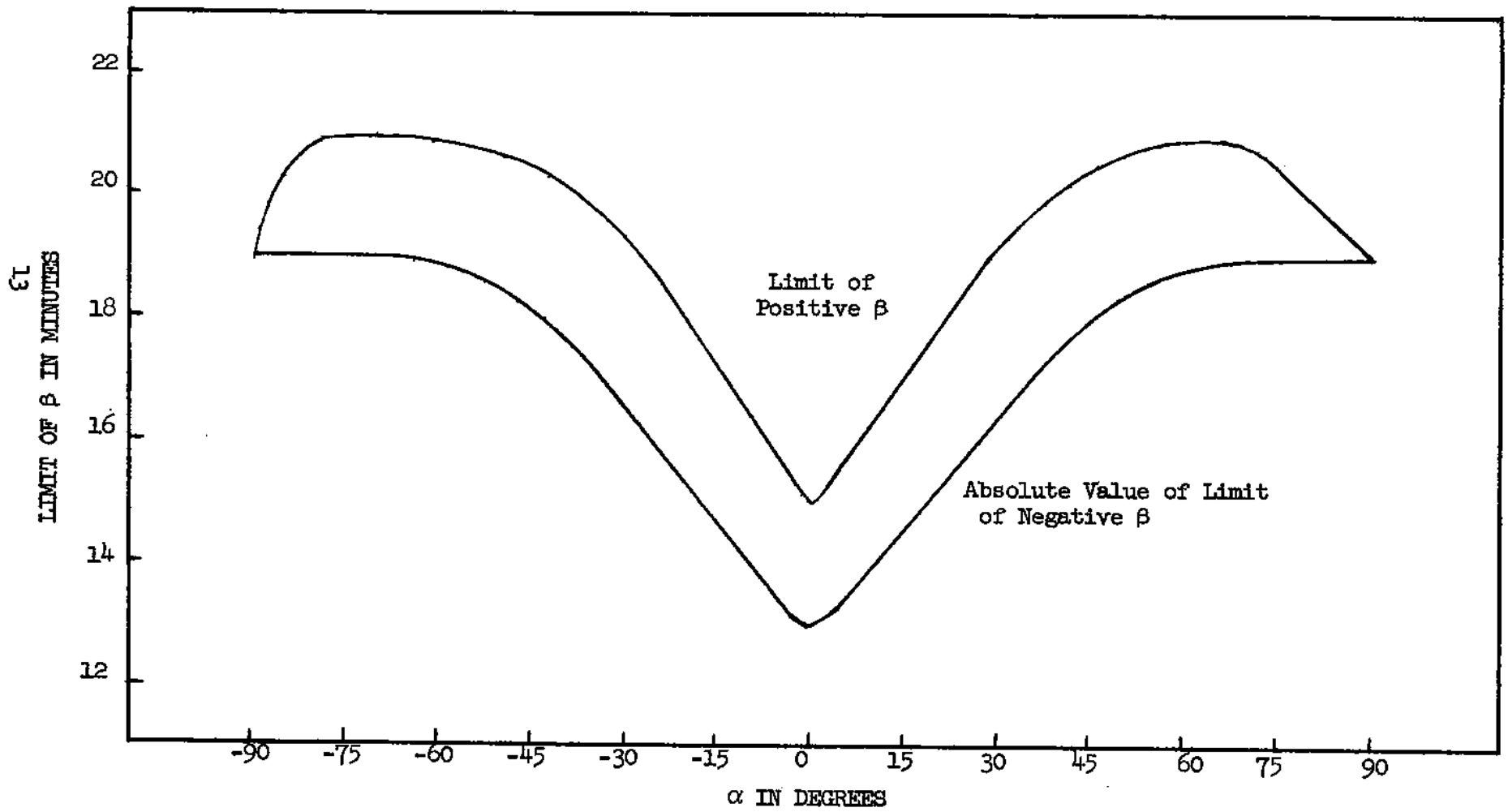

of this 3-digit number as a decimal between 0 and 1, then, for fixed α, β is determined by multiplying this number by the range of β corresponding to the given α and then adding this result to the minimum β.

A complete list of the ranges of β, the associated random 3-digit numbers and the values of beta corresponding to each α is given in Appendix I.

Numerical Example. Before proceeding to describing the procedure used to combine our 180 results we will work a numerical example to illustrate the estimation of the projected angle of obliquity given d, α, and the 3-digit scale factor. Let d = 100 feet, $\alpha = 30^{\circ}$ and the factor = 968. From Figure 5 we see the minimum β = -17' and the maximum is +19'. If we apply the scale factor we obtain $\beta = .968(36') + (-17') = 17'\ 50''$ to the nearest 10". We can now compute the intercepts of the specified trajectory, using the values: $\alpha = 30^{\circ}$, $\beta = 17'\ 50''$, and d = 100 feet = 1200 inches. The x-intercept, a, is found by the formula $a = d \sin \beta / \sin(\alpha + \beta)$ to be 12.35 inches, and the y-intercept $b = -a \tan(\alpha + \beta) = 7.22$ inches. These intercepts are then plotted on the graph paper, and the trajectory drawn through them. After drawing the tangent to the figure at the point of intersection of the trajectory, we find that the resultant angle of obliquity is 38°.

Combining and Smoothing the Data. We now have 180 angles of obliquity at each of two distances, 40 and 100 feet, and must combine them to obtain an estimate of their distribution. These 180 angles should not be given equal weight in determining the distribution; they should be weighted by their corresponding range of β. The reason for this is that the greater the range of β the greater the number of trajectories intersecting the inner figure. The weights used were the actual range of β in minutes. At 40 feet, these weights run from 70 to 100, and at 100 feet from 28 to 40. Because of the small variation in these weights, the effect of weighting on the distribution was small.

We next estimate the proportion of angles of obliquity less than or equal to, say, Ω, for $\Omega = 0^{\circ}$ to 65° in 5° increments. This is done by first arranging the 180 values for ω in increasing order with their corresponding weights β. Next add the 180 weights. The proportion of angles less than Ω is the sum of weights corresponding to angles $\omega \leq \Omega$ divided by the sum of all weights.

The final distribution is obtained by using standard mathematical procedures[4] to smooth the data. A 7-point smoothing formula was used for these data.

RESULTS

Table 2 contains a summary of the results of our study. The most important observation to be made is that, contrary to previous assumptions, the angles of obliquity are not clustered near zero. In fact the angles of obliquity are less than 5° in fewer than one-ninth of the cases. Also, as can be seen from the enumeration of all results in Appendix I, there are no angles of obliquity greater than 63°. This is the result of restricting our trajectories to those hitting the inner figure.

---

[4] Greville, Dr. T. N. E. "Adjusted Average Graduation Formulas of Maximum Smoothness". The Record, American Institute of Actuaries, Vol. XXXVI, Part II, No. 74, October 1947.

Greville, "Tables of Coefficients in Adjusted Average Graduation Formulas of Maximum Smoothness". The Record, American Institute of Actuaries, Vol. XXXVII, Part I, No. 75, April 1948.

Table 2. Cumulative Distribution of the Angles of Obliquity

at d = 40'	Per Cent of Angles Less than Given Value	
ω	Weighted Results	Smoothed Results
5	10.84	10.34
10	21.62	21.23
15	30.92	32.36
20	44.54	41.99
25	49.79	50.49
30	57.65	59.78
35	71.25	70.32
40	81.58	80.10
45	85.93	86.81
50	91.31	91.47
55	95.50	95.40
60	98.89	96.43
65	100.00	100.00
75	100.00	100.00
90	100.00	100.00

d = 100'	Per Cent of Angles Less than Given Value	
ω	Weighted Results	Smoothed Results
5	10.77	10.45
10	21.94	20.73
15	28.76	31.36
20	44.65	41.86
25	50.33	51.81
30	61.89	61.50
35	69.88	70.80
40	81.44	79.55
45	84.97	86.75
50	93.45	92.71
55	97.25	97.21
60	99.48	99.74
65	100.00	99.87
75	100.00	100.00
90	100.00	100.00

An approximation to the distribution of angles of obliquity is seen to be:

% of angles less than ω for ω between 0° and 40° = $(2\omega)\%$
" " " " " " " " " 40° and 60° = $(40 + \omega)\%$
" " " " " " " " " greater than 60° = 100%

DISCUSSION OF THE PROCEDURE

The most questionable aspect of our procedure is probably the use of a two-dimensional study for a three-dimensional problem. As previously noted, we are working with the projections of the actual angles onto the horizontal plane. However, we shall show that the differences between the projected angle and the true angle of obliquity are in most cases small so that our conclusion regarding the distribution of these angles should not be seriously affected by our use of projections.

Reference is made at this point to Figure 6. Angle ω in the horizontal plane is the projected angle of obliquity. Angle Φ is the true angle of obliquity, angle γ is the angle between the actual normal and its projection onto the horizontal plane, and angle μ is the angle between the actual trajectory and its projection. In general, if both the actual normal and trajectory are above the horizontal plane, these angles are related by the formula: $\cos \Phi = \sin \mu \sin \gamma + \cos \mu \cos \gamma \cos \omega$. This formula is derived in Appendix II. If they are on opposite sides of the horizontal plane the formula becomes: $\cos \Phi = \cos \mu \cos \gamma \cos \omega - \sin \mu \sin \gamma$. Using these formulas we computed the true angles of obliquity for a variety of combinations of the angles ω, μ, and γ. A summary of the results is contained in Figures 7 and 8.

Figure 6. The Projections

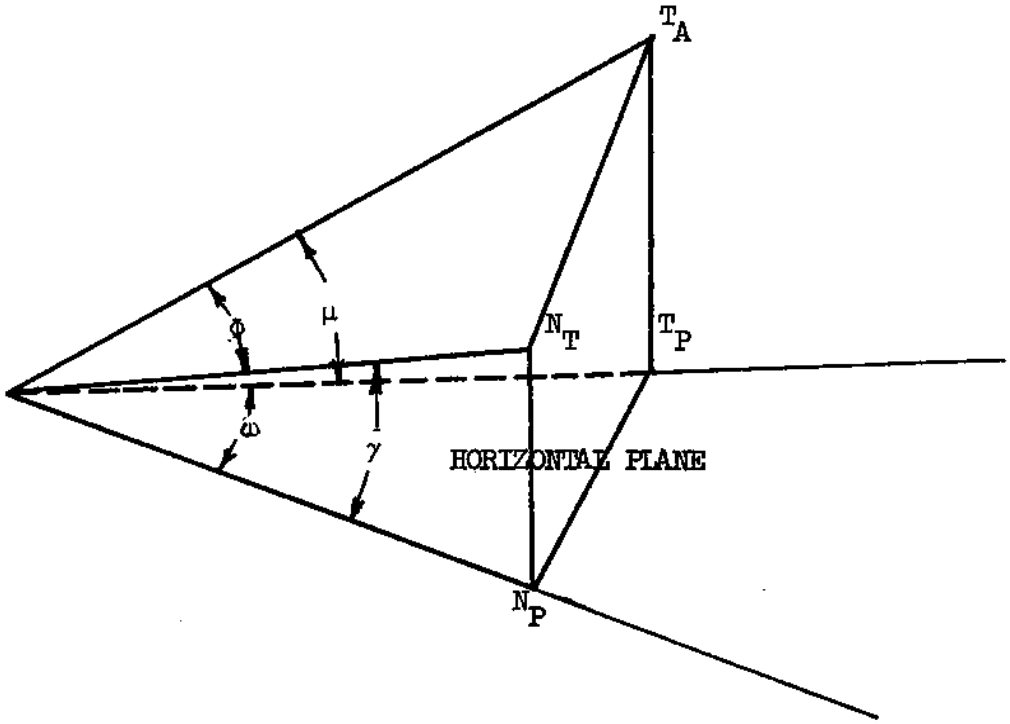

Figure 7. The Difference Between the Projected and True Angles of Obliquity When the Trajectory and Tangent are Both Above the Horizontal Plane

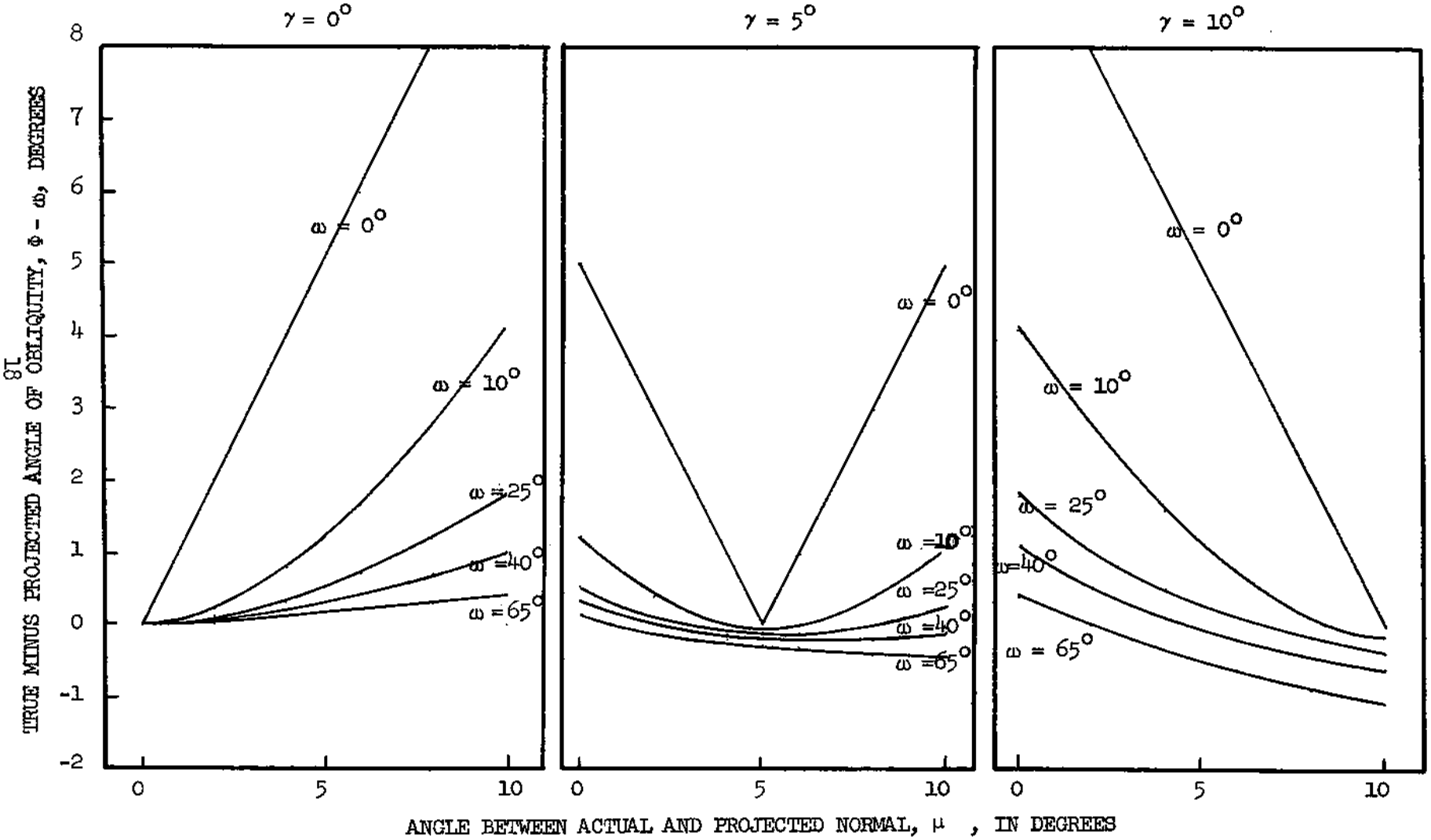

Figure 8. The Difference between the Projected and True Angles of Obliquity When the Trajectory and Tangent are on Opposite Sides of the Horizontal Plane

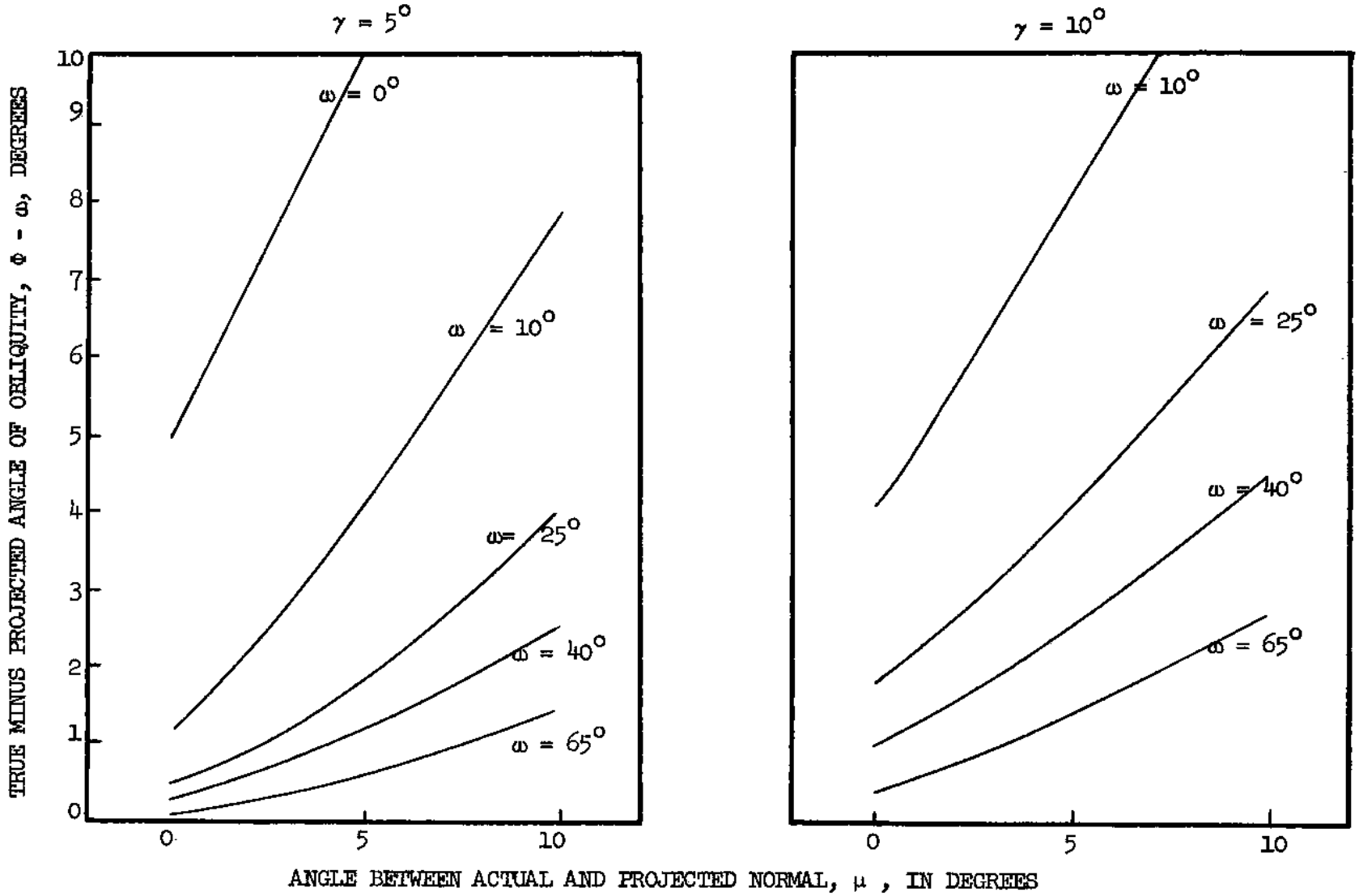

Note that the true angle of obliquity is, for the most part, greater than the projected angle and that for values of ω near 0°, the true angle of obliquity may be much greater than 0°. In this case, since the difference $\Phi - \omega$ is always positive we have underestimated the angle of obliquity and the effect on the actual distribution of the angles would be to shift the distribution toward the larger values of ω. Since cases of this sort can be expected to occur infrequently, we feel the conclusion arrived at using the distribution of projected angles is reasonably safe.

One final remark should be made concerning the charts -- note that the computations were made for values of μ and γ varying only from 0° to 10°. In considering the applications, this range is believed to be adequate. However, the conclusions regarding the relation of ω to Φ apply only for this range -- if the reader finds it necessary to compare these angles for other values of μ and γ, additional computations will be required.

In using our graphical method, human errors in drawing lines, measuring angles, and reproducing figures are bound to occur. For this reason, 19 measurements of the angles of obliquity were remade at each of the two distances. More specifically, after completing our 180 measurements at each distance, we repeated the entire graphical procedure for 19 of them. The angles to be remeasured were chosen in such a way that they were distributed evenly around the figure. In order to avoid being influenced by our earlier work, the remeasurements were remade several weeks after the original measurements. We found that the average absolute difference in measurements was $1\text{-}3/4^{\circ}$, with the largest difference being $4\text{-}3/4^{\circ}$. In some cases, both measurements were exactly the same. Table 3 contains a summary of these differences.

COMPARISON WITH RESULTS USING SIMPLER ASSUMPTIONS

A simpler approach to determining the distribution of the angles of obliquity has been proposed. The approach is to assume the target is elliptically shaped, with its major axis twice its minor one, and that the fragment trajectories are parallel and uniformly distributed, impinging only on the longer side of the ellipse. Since we found that the cross-section of the clothed man is appreciably larger than that of the unclothed man and that the ratio of the longer diameter of the target to its shorter one is more nearly 4 to 3 than 2 to 1, we used this information as well.

More specifically, we have obtained six additional sets of distributions of the angles of obliquity. Because they can be obtained easily, we did not hesitate to obtain distributions for all reasonable combinations

Table 3. The Differences Between Original and Second Measurements

Distance	Orig. Meas.	2nd Meas.	Difference Orig. - 2nd
40'	12° - 30'	13° - --	-0° - 30'
	55° - 30'	56° - 30'	-1° - --
	20° - --	24° - 45	-4° - 45'
	40° - --	42° - 30'	-2° - 30'
	33° - --	35° - 30'	-2° - 30'
	20° - 30'	17° - --	+3° - 30'
	22° - 30'	20° - --	+2° - 30'
	3° - --	7° - 30'	-4° - 30'
	36° - 15'	34° - --	+2° - 15'
	19° - 45'	19° - 30'	+0° - 15'
	14° - --	17° - 30'	-3° - 30'
	19° - --	18° - 15'	+0° - 45'
	19° - 30'	17° - 30'	+2° - --
	28° - 30'	27° - 30'	+1° - --
	7° - 45'	10° - 30'	-2° - 45'
	12° - --	13° - --	-1° - --
	23° - --	21° - --	+2° - --
	5° - --	5° - --	---
	57° - 30'	56° - 30'	+1° - --
100'	17° - 30'	19° - --	-1° - 30'
	16° - --	15° - --	+1° - --
	42° - --	46° - --	-4° - --
	29° - --	30° - --	-1° - --
	14° - --	18° - 30'	-4° - 30'
	39° - 30'	39° - --	+0° - 30'
	39° - 30'	35° - --	+4° - 30'
	3° - 30'	2° - --	+1° - 30'
	19° - --	16° - 30'	+2° - 30'
	35° - --	36° - --	-1° - --
	30° - 30'	30° - 30'	---
	17° - --	15° - 30'	+1° - 30'
	54° - 30'	53° - --	+1° - 30'
	35° - 30'	35° - --	+0° - 30'
	28° - 15'	28° - --	+0° - 15'
	8° - --	11° - --	-3° - --
	38° - --	40° - --	-2° - --
	49° - 30'	49° - --	+0° - 30'
	16° - 30'	16° - 30'	---

of simplifying assumptions. Thus three sets were obtained assuming the target is the ellipse itself, three others assuming the target is a second shape inside the ellipse. (Of course, as before, the angle of obliquity we seek is the angle made with the outer figure -- in this case the ellipse.) We assumed the axes of the inner target to be about three-quarters of those of the ellipse. The three sets obtained for each of these two targets were one using an ellipse with its major axis twice its minor one, a second with the ratio of its major axis to its minor one 4 to 3 and a third that incorporates trajectories impinging elsewhere than on the long side of the ellipse. For this third set we used a ratio of 4 to 3 (long side to short), obtained the distribution of the angle of obliquity assuming uniformly distributed, parallel trajectories impinging only on the short side and then combined these results with those obtained earlier for the long side. A weighted average was used to combine the two sets of results, "longs" with a weight of 4, "shorts", 3. Table 4 contains a summary of the six sets of results for angles of obliquity in 15° increments along with the two sets we had previously obtained using more realistic assumptions. A discussion of the results and a detailed description of how they were obtained follows.

Clearly a two by one ellipse won't do, using a 4 to 3 target improves the result considerably. However, even the third from last column, containing results obtained using the most realistic of the simplifying assumptions, misses the mark by putting too much in the range $0 - 15^{\circ}$ and too little in $30 - 60^{\circ}$. The only set of data not suffering from this defect, that for weighted results on a single target, puts so much less in the range $15 - 45^{\circ}$ and more in $60 - 90^{\circ}$ that it given an even poorer approximation overall.

We will now describe the procedure used to obtain the distribution using the simplifying assumptions. In general we will use $\frac{x^2}{c^2} + \frac{y^2}{e^2} = 1$ for the equation of the ellipse where c and e are the major and minor semi-axes, respectively. Because of the symmetry of the ellipse it is sufficient to consider just one quadrant. Consider Figure 8 below. Let AX_o be the trajectory of the fragment, intersecting the ellipse at B. Then, if BE is tangent to the ellipse at B and CB is normal to BE, we have ω = angle ABC is the angle of obliquity. But angle BCD = angle ABC and therefore cot ω = slope of BC. As is well known the slope of the normal is -dx/dy. Differentiating the formula for the ellipse implicitly with respect to y gives:

$$\frac{2x\,dx}{c^2}\,\frac{dx}{dy} + \frac{2y}{e^2} = 0 \quad \text{or} \quad \frac{-dx}{dy} = \frac{c^2}{e^2}\,\frac{y}{x}\,.$$

Table 4. Comparison of Results Using Simplifying Assumptions to those Using More Realistic Ones

Angle of Obliquity	Per Cent of Time Angle is Less Than Given One							
	Single Target			Imbedded Target			Realistic Model	
	2 to 1	4 to 3	Wted 4 to 3	2 to 1	4 to 3	Wted 4 to 3	D = 40'	D = 100'
15	47.2	33.6	27.6	62.2	44.4	36.6	30.9	28.8
30	75.6	60.8	51.7	100.0	80.5	68.7	57.6	61.9
45	89.4	80.0	71.4		100.0	94.6	85.9	85.0
60	96.1	91.8	86.4			100.0	98.9	99.5
75	99.1	98.0	96.4				100.0	100.0
90	100.0	100.0	100.0					

Hence, since points on the ellipse satisfy $y = \frac{e}{c}\sqrt{c^2 - x^2}$, we have

$$\cot \omega = \frac{c}{e}\sqrt{\frac{c^2 - x_o^2}{x_o}} \qquad \text{or}$$

$$x_o = \frac{c^2}{\sqrt{e^2 \cot^2 \omega + c^2}} \tag{1}$$

Figure 9. The Elliptical Target

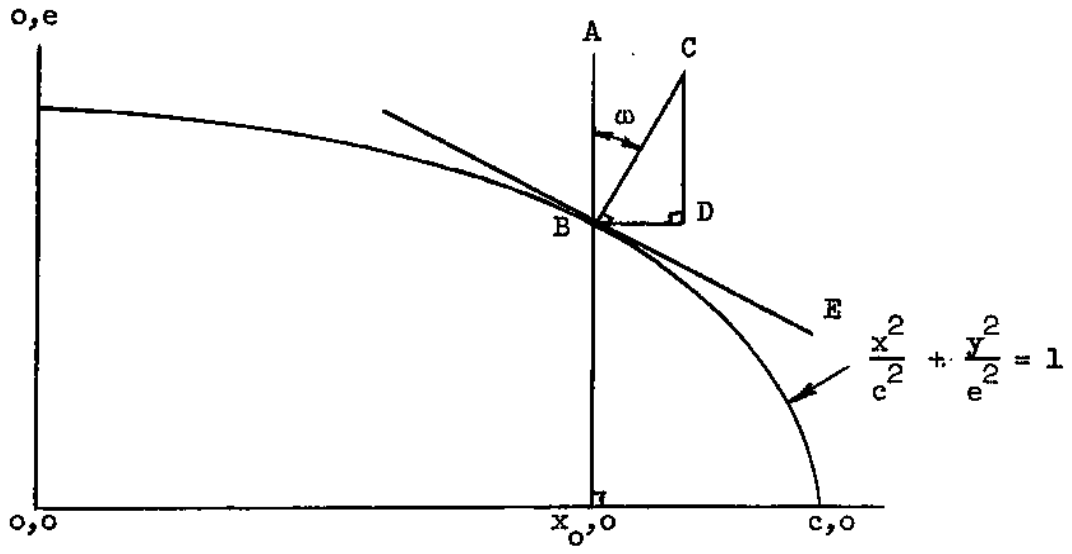

If the trajectories are parallel and uniformly distributed along the major axis of the ellipse, the cumulative distribution of the angles of obliquity is given by:

$$\text{Probability (the absolute value of the angle of obliquity} \leq \omega) = \frac{X_o}{c}$$

If we set $\omega = 15^\circ$, 30°, 45°, 60°, and 75°, we can get X_o using (1) and the corresponding cumulative probabilities.

Note that if we restrict our distribution to those actually hitting some imbedded target with a maximum semi-major-axis = $h < c$, then (assuming the trajectories proceed straight through the ellipse):

Probability (the absolute value of the angle of obliquity $\leq \omega$/a hit on the imbedded target) $= \frac{X_o}{h}$

Finally note that, by the symmetry in the ellipse, we may rewrite (1) to get the intercept on the short side of the ellipse, say,

$$y_o = \frac{e^2}{\sqrt{c^2 \cot^2 \omega + e^2}}$$

and now:

$$\text{prob. (and of obliquity} \leq \omega) = \frac{y_o}{e} \quad \text{or} \quad \frac{y_o}{g}$$

for the conditional probability if the maximum length of the semi-minor-axis of the imbedded figure is g. We proceed, as before, to get the cumulative distribution for $\omega = 15^o$, 30^o, 45^o, 60^o, and 75^o. Recall that the weighted results are obtained using:

$$\text{weighted result} = \frac{4\ (\text{result on long side}) + 3\ (\text{result on short side})}{7}$$

CONCLUSION

The distributions at both 40 and 100 feet indicate that the angles of obliquity cannot be assumed clustered near zero. In fact, for impacts on the upper torso at ranges of 40 to 100 feet, the proportion of these angles less than ω° is approximately $(2\ \omega)\%$ for ω between 0° and 40°, $(40 + \omega)\%$ for ω between 40° and 60°, and 100% for ω greater than 60°.

RECOMMENDATIONS

The distribution of angles of obliquity should be taken into consideration when assessing the effectiveness of body armor. More specifically the distributions presented in the report should be used in evaluating body armor protection for the upper torso at distances of 40 and 100 feet. The procedures presented herein can be used as required to estimate the distribution of the angles of obliquity that can be expected in attacks on other areas of the body.

APPENDIX I

The 180 Values of the Angles α and β Used in the Study and the Resultant Angles of Obliquity ω, for D = 40 Feet and D = 100 Feet

THE 180 VALUES OF THE ANGLES α AND β USED IN THE STUDY
AND THE RESULTANT ANGLES OF OBLIQUITY ω, FOR D = 40 FEET AND D = 100 FEET

D = 40 Feet						D = 100 Feet				
		β Range in Minutes		Random	α	Random	β Range in Minutes			
ω	β	Minimum	Maximum	Number	(In Degrees)	Number	Minimum	Maximum	β	ω
31°	34' 30"	-48	48	859	90	864	-19	19	13' 50"	29°
22°	22' 20"	-48	48	733	89	737	-19	19	9'	20°
37°	-39' 10"	-48	48	092	87	092	-19	19	-15' 30"	36°
35°	43'	-48	49	938	85	947	-19	19	17'	34°
21°	-19' 40"	-48	49	292	84	281	-19	19	- 8' 20"	18°
5°	- 40"	-48	49	488	83	488	-19	20	0' 00"	4°
23°	-23' 40"	-48	49	251	82	991	-19	20	19' 40"	37°
8°	- 4' 50"	-48	49	445	82	248	-19	20	- 9' 20"	20°
38°	-38' 30"	-48	50	097	81	098	-19	20	-15' 10"	38°
39°	49' 50"	-48	50	998	80	998	-19	20	20'	50°
20°	-19' 20"	-48	50	293	79	299	-19	20	- 7' 20"	19°
32°	-30' 30"	-48	50	179	78	196	-19	21	-11' 50"	29°
4°	10' 40"	-48	50	599	77	584	-19	21	4' 20"	8°
8°	14' 20"	-47	51	626	76	610	-19	21	5' 20"	8°
20°	-17' 50"	-47	51	298	75	296	-19	21	- 7' 10"	19°
28°	-25' 10"	-47	51	223	74	225	-19	21	-10'	28°
30°	41' 20"	-47	51	901	73	888	-19	21	16' 30"	27°
14°	24'	-47	52	717	72	312	-19	21	- 6' 30"	18°
20°	-16' 20"	-47	52	310	72	717	-19	21	9' 40"	14°
14°	23' 20"	-47	52	712	71	708	-19	21	9' 20"	13°
6°	14' 20"	-47	52	620	69	620	-19	21	5' 50"	7°
34°	-28' 30"	-48	52	195	68	192	-19	21	-11' 20"	32°
34°	-30'	-48	52	180	68	171	-19	21	-12' 10"	35°
4°	11'	-48	52	590	68	579	-19	21	4' 10"	4°
11°	22' 50"	-48	52	708	68	704	-19	21	9' 10"	13°

THE 180 VALUES OF THE ANGLES α AND β USED IN THE STUDY
AND THE RESULTANT ANGLES OF OBLIQUITY ω, FOR D = 40 FEET AND D = 100 FEET (Con't)

D = 40 Feet						D = 100 Feet				
		β Range in Minutes		Random	α	Random	β Range in Minutes			
ω	β	Minimum	Maximum	Number	(In Degrees)	Number	Minimum	Maximum	β	ω
20°	35' 10"	-47	52	830	67	825	-19	21	14'	23°
12°	22' 40"	-47	52	704	67	700	-19	21	9'	10°
54°	-44' 50"	-47	52	022	64	017	-19	21	-18' 20"	54°
12°	- 5' 20"	-47	52	421	63	421	-19	21	- 2' 10"	10°
28°	-21'	-47	52	263	62	271	-19	21	13'	28°
7°	3' 20"	-47	52	508	60	508	-19	21	1'	8°
16°	31' 20"	-47	52	791	59	796	-19	21	12' 50"	18°
11°	30' 10"	-47	52	779	58	783	-19	21	12' 20"	19°
11°	- 1' 30"	-47	52	459	57	459	-19	21	- 40"	10°
26°	-18'	-47	52	293	56	292	-19	21	- 7' 20"	26°
31°	39' 30"	-47	52	874	55	867	-19	21	15' 40"	31°
6°	6'	-47	52	535	54	538	-19	21	2' 30"	4°
38°	-30' 30"	-47	51	168	53	175	-19	21	-12'	37°
10°	25' 10"	-47	51	736	52	718	-18	21	10'	11°
38°	41' 50"	-47	51	906	51	893	-18	21	16' 50"	39°
19°	-11' 10"	-47	51	366	50	350	-18	21	- 4' 20"	18°
8°	3' 30"	-47	51	515	49	500	-18	21	1' 30"	8°
3°	14'	-47	51	622	48	607	-18	21	5' 40"	4°
16°	31' 10"	-47	51	798	47	789	-18	20	12'	20°
30°	-18' 10"	-46	51	287	46	282	-18	20	- 7'	27°
19°	30'	-46	51	784	45	784	-18	20	11' 50"	18°
18°	-10' 10"	-46	50	373	44	368	-18	20	- 4'	22°
28°	36' 30"	-46	50	859	43	855	-18	20	14' 30"	28°
36°	45' 40"	-46	50	955	42	956	-18	20	18' 20"	36°
32°	39' 30"	-45	50	889	41	886	-18	20	15' 40"	30°

THE 180 VALUES OF THE ANGLES α AND β USED IN THE STUDY
AND THE RESULTANT ANGLES OF OBLIQUITY ω, FOR D = 40 FEET AND D = 100 FEET (Con't)

D = 40 Feet						D = 100 Feet				
		β Range in Minutes		Random	α	Random	β Range in Minutes			
ω	β	Minimum	Maximum	Number	(In Degrees)	Number	Minimum	Maximum	β	ω
63°	-43' 40"	-45	50	014	40	461	-18	20	- 30"	16°
3°	20' 50"	-44	50	720	39	689	-18	20	8' 10"	9°
42°	-34' 40"	-44	50	099	38	099	-17	20	-13' 20"	50°
36°	-24'	-44	50	213	37	198	-17	20	- 9' 40"	35°
10°	21' 30"	-43	49	701	36	680	-17	20	8' 10"	5°
31°	-17' 40"	-43	49	276	35	276	-17	20	- 6' 50"	26°
56°	-38' 30"	-43	49	049	34	222	-17	19	- 9'	36°
35°	-22' 30"	-43	49	223	34	046	-17	19	-15' 20"	56°
23°	31' 10"	-42	48	813	32	813	-17	19	12' 20"	20°
44°	-28' 40"	-42	48	148	31	139	-17	19	-12'	46°
34°	44' 40"	-42	48	963	30	968	-17	19	17' 50"	38°
46°	-34' 40"	-42	48	081	30	074	-17	19	-14' 20"	52°
20°	- 50"	-41	47	456	29	444	-17	19	- 1'	19°
58°	-39' 10"	-41	47	020	28	020	-16	19	- 9'	37°
20°	25' 50"	-41	47	759	27	748	-16	19	10' 10"	16°
3°	13' 30"	-40	46	622	25	632	-16	18	5' 30"	4°
8°	3' 20"	-40	46	504	23	505	-16	18	1' 10"	10°
16°	- 1' 30"	-39	45	446	22	441	-16	18	- 1'	22°
28°	36'	-39	45	893	21	892	-16	18	14' 20"	26°
32°	40'	-38	45	940	20	934	-15	18	15' 50"	31°
14°	1' 20"	-38	44	480	19	479	-15	17	20"	12°
12°	23' 50"	-37	44	751	18	745	-15	17	8' 50"	11°
46°	42' 20"	-37	44	979	17	974	-15	17	16' 10"	41°
6°	12' 50"	-37	43	623	16	623	-15	17	5'	2°
36°	-16'	-37	43	262	15	359	-15	17	- 3' 30"	28°

THE 180 VALUES OF THE ANGLES α AND β USED IN THE STUDY
AND THE RESULTANT ANGLES OF OBLIQUITY ω, FOR D = 40 FEET AND D = 100 FEET (Con't)

D = 40 Feet						D = 100 Feet				
		β Range in Minutes		Random	α	Random	β Range in Minutes			
ω	β	Minimum	Maximum	Number	(In Degrees)	Number	Minimum	Maximum	β	ω
19°	29'	-36	43	823	14	823	-15	17	11' 20"	17°
4°	8' 30"	-36	42	571	12	559	-14	17	3' 20"	3°
20°	- 8' 30"	-36	41	357	11	357	-14	17	- 3'	16°
6°	2' 40"	-35	41	496	10	489	-14	16	40"	6°
16°	- 6'	-35	41	382	9	372	-14	16	- 2' 50"	18°
9°	17' 30"	-34	40	696	8	683	-14	16	6' 30"	9°
32°	-17'	-34	40	230	7	239	-14	16	- 6' 50"	32°
42°	-21' 30"	-34	39	171	6	172	-14	16	- 8' 50"	42°
40°	-21' 10"	-34	39	176	5	149	-13	16	- 8' 40"	41°
54°	-25' 50"	-33	39	100	4	092	-13	16	-10' 20"	47°
51°	-29'	-33	39	056	3	048	-13	15	-11' 40"	50°
11°	17' 50"	-33	38	716	2	720	-13	15	7' 10"	5°
3°	10' 10"	-33	37	617	1	613	-13	15	4' 10"	1°
44°	-23' 20"	-33	37	138	0	149	-13	15	- 8' 50"	44°
30°	-18' 30"	-33	37	207	- 1	214	-13	15	- 7'	29°
2°	9'	-33	38	592	- 2	595	-13	15	3' 40"	1°
2°	7' 40"	-33	39	566	- 3	566	-13	15	2' 50"	0°
2°	4' 30"	-33	39	521	- 4	518	-13	15	1' 30"	4°
48°	28'	-33	39	847	- 5	856	-13	16	11' 50"	46°
34°	19' 30"	-34	40	723	- 6	723	-13	16	8'	28°
54°	-31' 50"	-34	40	029	- 7	033	-14	16	-13'	54°
26°	30' 10"	-35	41	857	- 9	728	-14	16	7' 50"	29°
33°	20' 40"	-35	41	732	- 9	857	-14	16	11' 40"	48°
20°	-13' 20"	-35	41	285	-10	278	-14	16	- 5' 40"	19°
4°	5' 40"	-35	42	528	-11	528	-14	16	1' 50"	6°

THE 180 VALUES OF THE ANGLES α AND β USED IN THE STUDY
AND THE RESULTANT ANGLES OF OBLIQUITY ω, FOR D = 40 FEET AND D = 100 FEET (Con't)

D = 40 Feet						D = 100 Feet				
		β Range in Minutes		Random	α	Random	β Range in Minutes			
ω	β	Minimum	Maximum	Number	(In Degrees)	Number	Minimum	Maximum	β	ω
6°	- 10"	-36	42	459	-12	446	-14	17	- 10"	10°
46°	26' 50"	-36	42	806	-12	796	-14	17	10' 40"	46°
34°	-25' 30"	-36	42	135	-13	156	-15	17	-10'	33°
2°	6' 10"	-37	43	540	-15	540	-15	17	2' 20"	6°
4°	1'	-37	43	474	-16	474	-15	17	10"	6°
22°	10' 20"	-37	44	584	-17	594	-15	17	4'	21°
36°	-25' 30"	-37	45	140	-18	152	-15	18	- 9' 50"	30°
49°	26' 20"	-37	45	772	-19	758	-15	18	10'	46°
9°	4'	-38	45	506	-20	510	-15	18	1' 50"	12°
53°	-37' 40"	-38	46	004	-21	034	-16	18	-14' 50"	53°
29°	-24' 20"	-38	46	163	-22	897	-16	18	14' 30"	62°
63°	36' 30"	-38	46	887	-22	196	-16	18	- 9' 20"	29°
18°	6'	-39	47	523	-24	544	-16	18	2' 30"	24°
54°	28' 20"	-39	47	783	-24	804	-16	18	11' 20"	53°
46°	23'	-39	47	721	-25	735	-16	18	9'	46°
40°	-36'	-40	47	046	-26	033	-16	19	-14' 50"	42°
20°	3'	-40	48	489	-27	490	-16	19	1' 10"	16°
28°	-19' 20"	-40	48	234	-28	234	-16	19	- 7' 50"	29°
37°	-28' 40"	-40	48	129	-29	153	-17	19	-11' 30"	36°
44°	19' 50"	-41	49	676	-30	694	-17	19	8'	40°
22°	1' 40"	-41	49	474	-31	491	-17	19	40"	22°
35°	-27' 40"	-41	49	148	-32	537	-17	19	2' 20"	26°
27°	7' 20"	-41	49	537	-32	854	-17	19	13' 40"	56°
58°	35' 50"	-41	49	854	-32	148	-17	19	-11' 40"	38°
14°	-15' 50"	-42	49	287	-34	287	-17	20	- 6' 20"	16°

THE 180 VALUES OF THE ANGLES α AND β USED IN THE STUDY
AND THE RESULTANT ANGLES OF OBLIQUITY ω, FOR D = 40 FEET AND D = 100 FEET (Con't)

D = 40 Feet						D = 100 Feet				
		β Range in Minutes		Random	α	Random	β Range in Minutes			
ω	β	Minimum	Maximum	Number	(In Degrees)	Number	Minimum	Maximum	β	ω
34°	12' 10"	-42	50	589	-35	604	-17	20	5' 20"	36°
58°	44' 20"	-42	50	938	-36	946	-17	20	18'	58°
43°	22' 50"	-43	50	708	-37	719	-18	20	9' 20"	47°
56°	42' 10"	-44	50	916	-38	918	-18	20	16' 50"	55°
46°	-36' 50"	-44	50	076	-39	083	-18	20	-14' 50"	46°
50°	29' 50"	-44	50	785	-40	781	-18	20	11' 40"	49°
56°	48'	-44	50	979	-41	974	-18	20	19'	56°
40°	-31' 30"	-45	50	142	-42	140	-18	20	-12' 40"	38°
8°	-10' 40"	-45	50	361	-43	368	-18	20	- 4'	12°
54°	47' 50"	-45	51	967	-45	987	-18	20	19' 30"	54°
49°	38' 30"	-45	51	870	-45	890	-18	20	15' 50"	49°
42°	26' 30"	-45	51	745	-46	781	-18	20	10' 40"	42°
34°	14' 50"	-46	51	627	-47	623	-18	20	5' 40"	34°
12°	- 7' 40"	-46	52	391	-48	386	-18	20	- 3' 20"	11°
51°	-41'	-46	52	051	-49	047	-18	21	-16' 50"	48°
28°	15' 10"	-47	51	634	-50	620	-18	21	6' 10"	33°
40°	31' 20"	-47	51	799	-51	769	-18	21	12'	40°
37°	19' 40"	-47	51	680	-51	675	-18	21	8' 20"	40°
10°	-25'	-48	52	230	-54	214	-18	21	- 9' 40"	8°
34°	21	-48	52	690	-56	675	-18	21	8' 20"	34°
44°	45' 40"	-48	52	937	-57	089	-19	21	-15' 30"	40°
40°	-39' 10"	-48	52	089	-57	937	-19	21	18' 30"	44°
46°	48' 20"	-48	52	963	-58	954	-19	21	19' 10"	46°
7°	-14' 40"	-48	52	333	-59	450	-19	21	- 1'	18°
4°	-18' 10"	-48	52	298	-59	325	-19	21	- 6'	7°

THE 180 VALUES OF THE ANGLES α AND β USED IN THE STUDY
AND THE RESULTANT ANGLES OF OBLIQUITY ω, FOR D = 40 FEET AND D = 100 FEET (Con't)

D = 40 Feet						D = 100 Feet				
		β Range in Minutes		Random	α	Random	β Range in Minutes			
ω	β	Minimum	Maximum	Number	(In Degrees)	Number	Minimum	Maximum	β	ω
14°	-29'	-48	52	190	-59	196	-19	21	-11' 50"	10°
17°	- 2'	-48	52	460	-59	287	-19	21	- 7' 30"	0°
31°	27' 20"	-48	52	753	-61	742	-19	21	10' 40"	30°
39°	42' 20"	-48	52	903	-62	892	-19	21	16' 40"	37°
33°	35' 50"	-48	52	839	-64	229	-19	21	- 9' 50"	3°
9°	-30'	-48	52	180	-64	839	-19	21	14' 30"	32°
15°	- 3' 40"	-48	52	443	-65	433	-19	21	- 1' 40"	14°
35°	42' 50"	-48	52	908	-67	912	-19	21	17' 30"	36°
30°	-42' 50"	-48	52	051	-68	051	-19	21	1' 20"	18°
21°	15' 50"	-48	51	645	-69	646	-19	21	6' 50"	21°
26°	31' 20"	-48	51	801	-70	792	-19	21	12' 40"	26°
19°	20'	-48	51	687	-71	671	-19	21	7' 50"	22°
1°	-20'	-48	50	286	-72	271	-19	21	- 8' 10"	2°
24°	35' 50"	-48	50	855	-73	855	-19	21	15' 10"	18°
38°	48' 40"	-48	50	986	-74	971	-19	21	19' 50"	40°
8°	-28' 10"	-48	50	202	-75	196	-19	21	-11' 10"	7°
4°	-21' 10"	-48	50	274	-76	258	-19	21	- 8' 40"	2°
20°	30' 50"	-48	50	804	-77	775	-19	21	12'	20°
4°	-13' 50"	-48	50	349	-78	329	-19	21	- 5' 50"	1°
5°	- 8' 40"	-48	50	401	-79	382	-19	21	- 3' 40"	4°
18°	-37' 10"	-48	50	111	-80	112	-19	21	-14' 30"	17°
24°	44'	-48	50	938	-81	938	-19	21	18' 30"	34°
22°	33' 50"	-48	49	844	-82	812	-19	21	13' 30"	21°
33°	47'	-48	49	979	-82	942	-19	21	18' 40"	31°
18°	30' 50"	-48	49	813	-84	800	-19	21	13'	19°

THE 180 VALUES OF THE ANGLES α AND β USED IN THE STUDY
AND THE RESULTANT ANGLES OF OBLIQUITY ω, FOR D = 40 FEET AND D = 100 FEET (Con't)

D = 40 Feet						D = 100 Feet				
		β Range in Minutes		Random	α	Random	β Range in Minutes			
ω	β	Minimum	Maximum	Number	(In Degrees)	Number	Minimum	Maximum	β	ω
23°	38'	-48	49	887	-85	850	-19	21	15'	22°
12°	25' 20"	-48	48	764	-87	744	-19	20	10'	11°
19°	35' 20"	-48	48	868	-88	855	-19	20	14' 20"	18°
14°	29'	-48	48	807	-89	807	-19	19	11' 40"	15°
4°	11' 30"	-48	48	620	-90	620	-19	19	4' 30"	4°

APPENDIX II

Mathematical Development of the Relationship

$$\cos \Phi = \cos \omega \cos \mu \cos \gamma + \sin \mu \sin \gamma$$

where: Φ = true angle of obliquity

ω = projected angle of obliquity

μ = angle between the true normal and the horizontal plane

γ = angle between the true trajectory and the horizontal plane

In this Appendix we will establish the formula relating the true angle of obliquity to the projected angle. To do this we require Figure 6 which is given again below as Figure 10 with some change in the notation to facilitate the presentation of the arguments.

Figure 10. The Projections

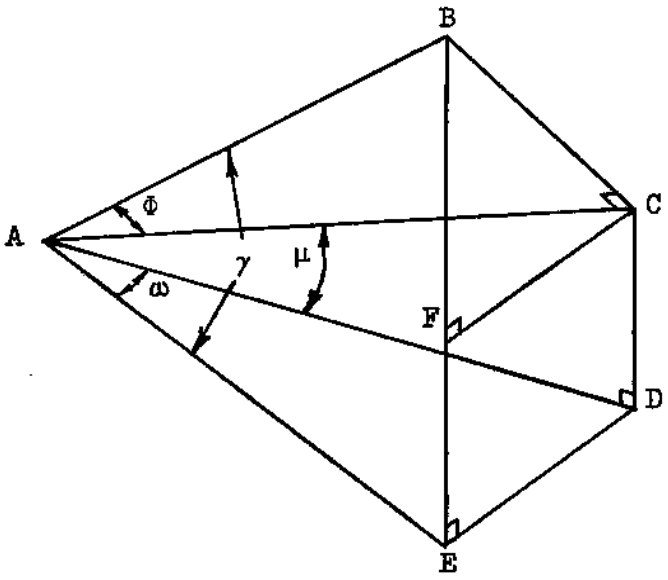

△ AED LIES IN THE HORIZONTAL PLANE, A IS THE POINT OF IMPACT

If we let AB be the trajectory and AC be the normal, then the angle Φ is the true angle of obliquity. First, we can pick any point B on the trajectory and construct BC perpendicular to AC. From C we then drop CD, and from B drop BE, perpendicular to the horizontal plane (AED). Then ω is the projected angle of obliquity. Finally, we draw FC parallel to ED.

From triangle AED (which is not necessarily a right triangle) using the law of cosines we get: $\cos \omega = \dfrac{\overline{AE}^2 + \overline{AD}^2 - \overline{ED}^2}{2\,\overline{AE}\,\overline{AD}}$. From $\overline{AD}^2 + \overline{DC}^2 = \overline{AC}^2$ and $\overline{AE}^2 + \overline{BE}^2 = \overline{AB}^2$ we get $\overline{AD}^2 + \overline{AE}^2 = \overline{AB}^2 + \overline{AC}^2 - \overline{DC}^2 - \overline{BE}^2$ and since $(\overline{BE} - \overline{DC})^2 + \overline{ED}^2 = \overline{BC}^2$, we get $-2\,\overline{BE}\,\overline{CD} - \overline{BC}^2 = -\overline{BE}^2 - \overline{DC}^2 - \overline{ED}^2$. Combining these two and substituting in the equation for $\cos \omega$, we find that:

$\cos \omega = \dfrac{\overline{AB}^2 + \overline{AC}^2 - 2\,\overline{BE}\,\overline{CD} - \overline{BC}^2}{2\,\overline{AE}\,\overline{AD}}$. But $\overline{AB}^2 = \overline{AC}^2 + \overline{BC}^2$ so

$\cos \omega = \dfrac{\not{2}\,(\overline{AC}^2 - \overline{BE}\,\overline{CD})}{\not{2}\,\overline{AE}\,\overline{AD}} = \dfrac{\overline{AC}}{\overline{AD}}\,\dfrac{\overline{AC}}{\overline{AB}}\,\dfrac{\overline{AB}}{\overline{AE}} - \dfrac{\overline{BE}}{\overline{AE}}\,\dfrac{\overline{CD}}{\overline{AD}}$. In terms of trigonometric functions, we get: $\cos \omega = \dfrac{1}{\cos \mu} \cdot \dfrac{\cos \Phi}{1} \cdot \dfrac{1}{\cos \gamma} - \tan \cdot \tan \mu$.

Equivalently, $\cos \omega = \dfrac{\cos \Phi - \sin \mu \sin \gamma}{\cos \mu \cos \gamma}$ and finally we obtain

$\cos \Phi = \cos \omega \cos \mu \cos \gamma + \sin \mu \sin \gamma$.

DISTRIBUTION

# Copies	
1	Assistant Secretary of Defense (Installations & Logistics) Washington 25, D. C.
1	Development Branch Research & Engineering Division Office of The Quartermaster General
1	QM Historian Office of The Quartermaster General Washington 25, D. C.
5	Personnel Armor Branch Chemicals and Plastics Division QM Research & Engineering Center Laboratories Natick, Massachusetts
4	Commanding Officer Ballistic Research Laboratories Aberdeen Proving Ground, Maryland ATTN: Keith Myers (2) Joseph Sperraza (1) I. J. Dunn, Jr. (1)
2	Commanding Officer U.S. Army Chemical Warfare Laboratories Edgewood, Maryland ATTN: George N. Stuart
2	Director, U. S. Naval Research Laboratory Washington 25, D. C. ATTN: Dr. Sanford P. Thompson, Code 4530 (1) Major T. J. Snipes, Code 1073 (1)
1	Chief, Operations Research Division Army Research Office Arlington Hall Station Arlington 12, Virginia
1	Dr. I. R. Hershner Chief, Physical Sciences Division Army Research Office Arlington Hall Station Arlington 12, Virginia

# Copies	
3	British Joint Services Mission (Army Staff) British Embassy Annexe Washington 8, D. C.
10	Commander Armed Services Technical Information Agency Arlington Hall Station Arlington 12, Virginia
1	The Army Library Room 1A 518 The Pentagon Washington 25, D. C.

AD 255237

Office of The Quartermaster General Department of the Army, Wash. 25,D.C.

A SET OF ANGLES OF OBLIQUITY FOR USE IN ASSESSING BODY ARMOR by Herbert Maisel, Wallace Chandler, Gerald DeCarlo.

Unclassified report

Measures of the effectiveness of body armor have been obtained in the past assuming the angle of obliquity is zero, i.e., that the projectiles strike the armor normal to its surface. Since penetrability is a function of the angle of obliquity, it is important to determine the set of angles likely to be encountered and to use this set when

(over)

UNCLASSIFIED

1. Body Armor - Obliquity
2. Numerical Methods and Procedures - Monte Carlo Method

I. Title: Distribution of Obliquities

II. Title: Evaluating Body Armor

III. Title: Smoothing Distributions

(over)

AD

Office of The Quartermaster General Department of the Army, Was. 25, D.C.

A SET OF ANGLES OF OBLIQUITY FOR USE IN ASSESSING BODY ARMOR by Herbert Maisel, Wallace Chandler, Gerald DeCarlo.

Unclassified report

Measures of the effectiveness of body armor have been obtained in the past assuming the angle of obliquity is zero, i.e., that the projectiles strike the armor normal to its surface. Since penetrability is a function of the angle of obliquity, it is important to determine the set of angles likely to be encountered and to use this set when

(over)

UNCLASSIFIED

1. Body Armor - Obliquity
2. Numerical Methods and Procedures - Monte Carlo Method

I. Title: Distribution of Obliquities

II. Title: Evaluating Body Armor

III. Title: Smoothing Distributions

(over)

AD

Office of The Quartermaster General Department of the Army, Wash. 25,D.C.

A SET OF ANGLES OF OBLIQUITY FOR USE IN ASSESSING BODY ARMOR by Herbert Maisel, Wallace Chandler, Gerald DeCarlo.

Unclassified report

Measures of the effectiveness of body armor have been obtained in the past assuming the angle of obliquity is zero, i.e., that the projectiles strike the armor normal to its surface. Since penetrability is a function of the angle of obliquity, it is important to determine the set of angles likely to

(over)

UNCLASSIFIED

1. Body Armor - Obliquity
2. Numerical Methods and Procedures - Monte Carlo Method

I. Title: Distribution of Obliquities

II. Title: Evaluating Body Armor

III. Title: Smoothing Distributions

(over)

AD

Office of The Quartermaster General Department of the Army Wash. 25,D.C.

A SET OF ANGLES OF OBLIQUITY FOR USE IN ASSESSING BODY ARMOR by Herbert Maisel, Wallace Chandler, Gerald DeCarlo.

Unclassified report

Measures of the effectiveness of body armor have been obtained in the past assuming the angle of obliquity is zero, i.e., that the projectiles strike the armor normal to its surface. Since penetrability is a function of the angle of obliquity, it is important to determine the set of angles likely to be encountered and to use this set when

(over)

UNCLASSIFIED

1. Body Armor - Obliquity
2. Numerical Methods and Procedures - Monte Carlo Method

I. Title: Distribution of Obliquities

II. Title: Evaluating Body Armor

III. Title: Smoothing Distributions

(over)